

Effectively Paralleling Gallium Nitride Transistors for High Current and High Frequency Applications



David Reusch, Ph.D., Director of Applications Engineering

Gallium nitride (GaN) based power devices are rapidly being adopted due to their ability to operate at frequencies and switching speeds beyond the capability of silicon (Si) power MOSFETs. In this application note, we will discuss paralleling high speed GaN transistors in applications requiring higher output current. This work will discuss the impact of in-circuit parasitics on performance and propose printed circuit board (PCB) layout methods to improve parallel performance of high speed GaN transistors. Four parallel half bridges in an optimized layout operated as a 48 V to 12 V, 480 W, 300 kHz, 40 A single phase buck converter achieving efficiencies above 96.5% from 35% to 100% load will be demonstrated.

Power converters are constantly trending towards higher output power, higher efficiency, higher power density, higher temperature operation, and higher reliability, all while providing a lower overall system cost. To provide improved performance better power devices are required. For silicon (Si) power devices, the gains in performance have slowed as the technology has matured and approaches its theoretical limits. Gallium nitride (GaN) transistors have emerged as a possible replacement for silicon devices in various power conversion applications and as an enabler of new applications not previously possible [1].

Since the first commercially available enhancement mode gallium nitride transistors were launched in 2010, eGaN FETs have had extremely low on-resistance in an extremely small footprint compared with any previously available semiconductor. As shown in figure 1, eGaN FETs are continuing this tradition with the latest generations of GaN devices, which have a lateral device structure and voltages ranging from 15-300 V. At 200 V, the eGaN FET has a specific on-resistance, which is the product of the device area and on-resistance, 9.5 times lower than the best state of the art MOSFET. At voltages of 100 V, 80 V, 60 V, and 40 V, eGaN FETs provide

respective specific on-resistance reductions of 2.4, 2.2, 1.6, and 1.05 times that of the best state of the art MOSFETs.

GaN technology, in its early stages, is far from its theoretical limit [1] and the rate of improvement in GaN has been, and will continue to be rapid.

While reducing the specific on-resistance of a transistor can increase the amount of current that can be conducted in a given area, it does not directly correlate to superior in-circuit performance, especially for high frequency power converter design where switching losses are often the dominant loss mechanism. Switching figures of merit (FOM) [2]-[8] have been used for almost half a century to compare the in-circuit performance capability of a given device technology in different applications. A popular FOM is the gate charge FOM [6], which is shown in figure 2 for eGaN FETs and state of the art MOSFETs. At voltages of 200 V, 100 V, and 40 V, eGaN FETs provide respective specific on-resistance reductions of 9, 5.5, and 1.9 times that of the best state of the art MOSFETs. There are various FOMs derived for different applications such as hard-switching applications and resonant and soft-switching applications [9].

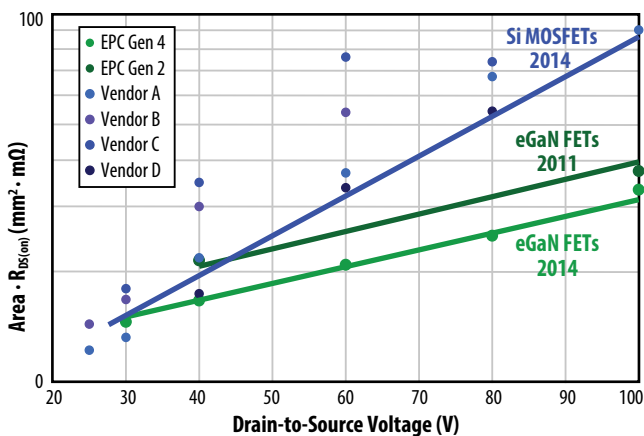


Figure 1: Specific on-resistance vs. blocking voltage capability for silicon MOSFETs and eGaN FETs.

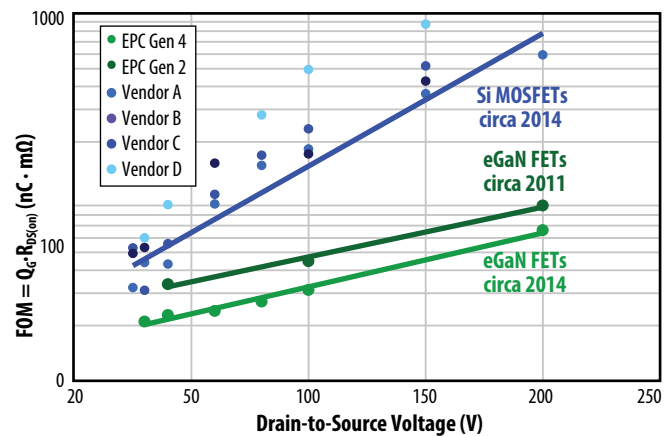


Figure 2: Gate charge FOM comparison of eGaN FETs and state-of-the-art Si MOSFETs for drain-to-source voltages at half of their rated voltage and a drain-to-source current of 20 A.

GaN transistors provide lower FOMs for all applications and this translates into significant performance improvements when compared to state of the art Si MOSFETs over a wide range of applications [9]-[14].

While FOMs are valuable tools to compare device technologies, the in-circuit performance is also greatly influenced by parasitics, including both package and printed circuit board (PCB) layout parasitics. In this application note, we will evaluate the impact of parasitics on performance and then assess the ability to parallel high speed GaN transistors for higher power applications. A method to improve the parallel performance of GaN transistors will be proposed and experimentally verified for four parallel half bridges operated as a 48 V to 12 V, 480 W, 300 kHz, 40 A single phase buck converter.

Impacts of parasitics on performance

In practical applications, lower FOM is just one of the contributors to achieving higher efficiency. In a buck converter, there are two major parasitic inductances that have a significant impact on converter performance as shown in figure 3. The common source inductance, L_s , is the inductance shared by the drain-to-source power current path and gate driver loop. The high frequency power loop inductance, L_{loop} , is the inductance in the device commutation loop, which is comprised of the parasitic inductance from the positive terminal of the input capacitance, through the top device, synchronous rectifier, ground loop, and input capacitor.

The common source inductance, L_s , has been shown to be critical to performance because it directly impacts the driving speed of the devices [15], [16]. As common source inductance increases, the effective gate drive voltage and gate drive current are significantly reduced, slowing switching speeds and increasing switching losses as described in equation (1). The impact of inductance

on a switching transition can be seen as part of the parasitic di/dt voltage bump on the Si MOSFET waveform shown in figure 4. The available gate drive current at turn-on is given by:

$$I_G = \frac{V_{Driver} - V_{GS} - V_{L_s}}{R_G} = \frac{V_{Driver} - V_{GS} - L_s \cdot \frac{di_{DS}}{dt}}{R_G} \quad (1)$$

Where V_{Driver} is gate drive voltage, V_{GS} is the gate to source voltage across the device, V_{L_s} is the effective voltage across the common source inductance, which is equal to $L_s \cdot di_{DS}/dt$ during device current

commutation, and R_G is the effective gate resistance including the driver resistance, the internal power device resistance, and external gate loop resistance.

The high frequency loop inductance, L_{loop} , while not as penalizing to switching speeds as common source inductance, still negatively impacts switching performance [17], [18]. Another major drawback of high frequency loop inductance is the drain-to-source voltage spike induced during the switching transition, shown in figure 4, given by:

$$V_{L_{LOOP}} = L_{LOOP} \cdot \frac{di_{DS}}{dt} \quad (2)$$

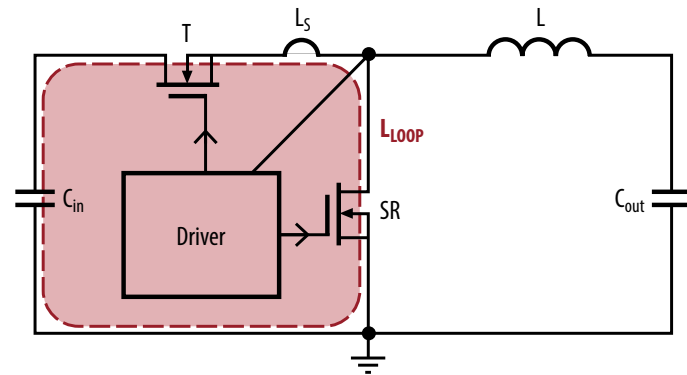


Figure 3: Synchronous buck converter with parasitic inductances.

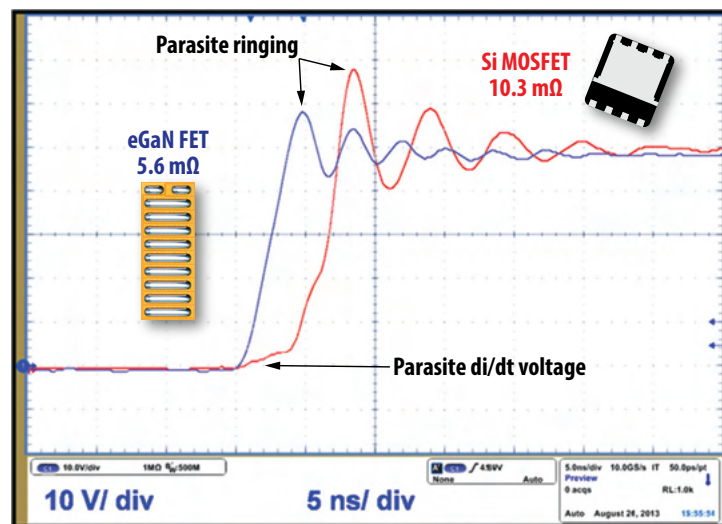


Figure 4: Switching node waveforms of eGaN FET and MOSFET designs ($V_{IN} = 48$ V, $I_{OUT} = 10$ A, $f_{sw} = 300$ kHz, GaN transistors: EPC2001 MOSFETs: BSZ123N08NS3G).

A. Package parasitics

To enable the high switching speed available from the low FOM of GaN transistors, low parasitic packaging and printed circuit board (PCB) layout is required. This subsection will compare the device packaging of GaN transistors and Si MOSFETs.

For Si trench MOSFET structures, the gate and source terminals and the drain terminal are located on opposite sides of the device. This forces an external connection from either the source and gate or the drain to connect the device to the PCB, introducing performance limiting package parasitics. The Loss Free Package (LFPACK), one of the most common packages for Si devices, is shown in figure 5. The LFPACK uses an external lead frame to connect the source and gate terminals to the PCB. The source connection of the LFPACK introduces over 0.5 nH of common source inductance alone, degrading the in-circuit performance of the Si MOSFET power device [11].

The high voltage lateral GaN transistor in a Land Grid Array (LGA) package has a major packaging advantage because all of the connections are located on the same side of the die, as shown in figure 6, eliminating the requirement of complex high-parasitic packaging. The LGA GaN transistor has a total package inductance estimated to be under 0.2 nH, significantly lower than any Si MOSFET package. In [10], the impact of the GaN transistor LGA package and the reduction of package parasitic inductance and resistance over the best available trench devices are quantified.

B. Printed circuit board parasitics

With higher switching speeds and lower package parasitic inductances the printed circuit board layout can become the limiting factor in converter performance. The most critical parasitic to reduce is the common source inductance, which is the inductance shared by the high frequency power loop and gate driver loop. To minimize the common source inductance added by PCB layout it is recommended to locate the gate driver loop and high frequency power loop where they have very little interaction. An example layout is shown in figure 7, where the gate drive loop, shown in red, and the high frequency loop, shown in yellow, interact only directly next to the GaN transistor, minimizing the common source inductance to the ultra-low internal package inductance offered by the GaN transistor package.

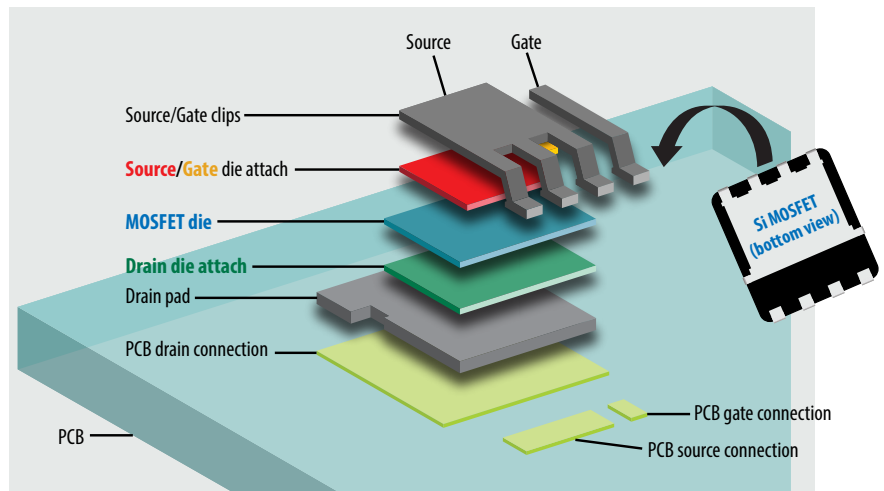


Figure 5: Exploded view of Si MOSFET Loss Free Package (LFPACK).

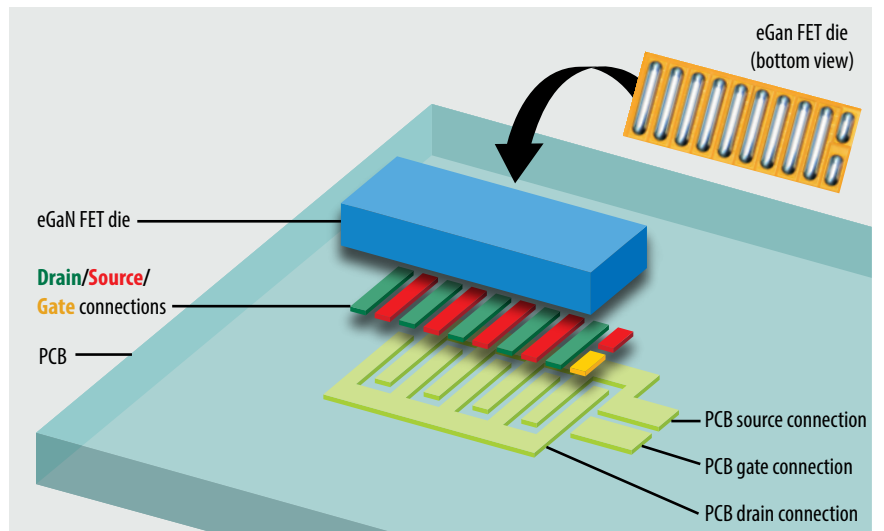


Figure 6: Exploded view of eGaN FET Land Grid Array package (LGA).

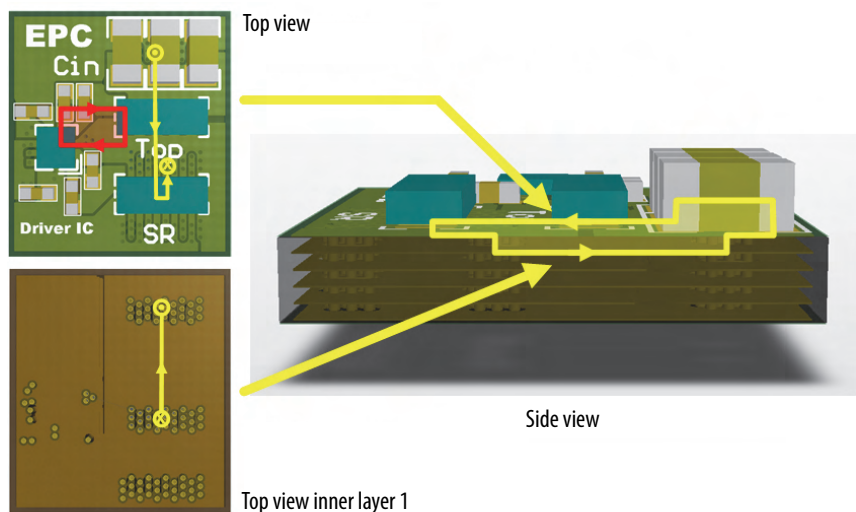


Figure 7: Optimal power loop with eGaN FETs top view, top view of inner layer 1, and side view.

To reduce the high frequency loop inductance over conventional designs an optimal layout was developed that utilizes the first inner layer, shown in the bottom left of figure 7, as a power loop return path. This return path is located directly underneath the top layer's power loop path, shown in the upper left of figure 7, allowing for the smallest physical loop size and providing magnetic field self-cancellation. The side view, shown in figure 7 illustrates the concept of creating a low profile magnetic field self-cancelling loop in a multilayer PCB structure. By using the optimal layout developed by EPC, GaN based half bridge designs have achieved high frequency loop inductances below 0.4 nH [18], further improving the in-circuit performance of GaN transistors when compared to Si MOSFETs.

Combining lower FOM, lower package parasitics, and lower parasitic PCB layouts, GaN transistors provide significant performance benefits over state of the art Si technology. GaN transistors have the ability to improve switching speeds with smaller, lower on-resistance devices as shown in figure 4. This allows for circuit designers to achieve lower dynamic switching losses and lower static conduction losses resulting in significantly reduced device loss and higher system efficiency.

Improving high speed GaN transistors parallel performance

The previous section demonstrated enhanced performance with single GaN transistors. In many applications, higher current is required. In this section, we will evaluate the ability to parallel GaN transistors to provide high efficiency in high output current applications.

A. Challenges of paralleling high speed GaN transistors

The objective of paralleling devices is to combine multiple higher on-resistance devices to appear and operate as a single, lower on-resistance device allowing for higher power handling capability. To effectively parallel devices, each device should equally share current dynamically, and in steady state, and equally divide switching related losses. The introduction of unbalanced in-circuit parasitics between parallel devices leads to uneven sharing and degraded electrical and thermal performance, limiting the effectiveness of paralleling devices [19]. For high speed devices such as GaN transistors, the increased switching speeds amplify the impact of parasitic mismatches [20].

In the previous section, the importance of minimizing common source inductance and high frequency loop inductance were addressed. For paralleling GaN transistors, these parasitics must not only be minimized to achieve the best performance but also need to be balanced to ensure proper parallel operation. As the difference between the common source and high frequency loop inductance increases between the parallel half bridges, so does the dynamic current difference:

$$I_{DIFF} = \frac{I_{SW1} - I_{SW2}}{I_{SW1} + I_{SW2}} \quad (3)$$

Where I_{DIFF} is the dynamic current difference between the two parallel GaN half bridges and I_{SW1} and I_{SW2} are the respective currents in the parallel transistors when the output current (I_{OUT}) is reached after a switching transition.

To evaluate the impact of parasitics on current sharing, a simulation was created using 100 V EPC2001 models in LTSPICE. Figure 8 shows how current sharing worsens with parasitic imbalance in the high frequency loop inductance for two parallel GaN half bridges (nominal drain inductance ($L_D = L_{LOOP} - L_S$) was set to 0.3 nH and increased in only one of the half bridge pairs) operating at 48 V with various common source inductances, where the common source inductance was kept the same for both of the parallel half bridges. From figure 8 it can also be observed that as the common source inductance decreases, current sharing issues become more pronounced. The magnified current sharing issues at lower common source inductance values are generated by higher switching speeds. As the current sharing worsens between parallel devices the electrical and thermal performance degrades as we will show in the following section.

The current sharing difference resulting from parasitic imbalance in the common source inductance for two parallel GaN half bridges operating at 48 V for various high frequency loop inductances is shown in figure 9 (nominal common source inductance was set to 0.1 nH and increased in only one of the half bridge pairs and drain inductance was kept the same for both of the parallel half bridges). Similar to loop inductance imbalance, as common source inductance varies, current sharing worsens. This trend is magnified as loop inductance decreases and capable switching speeds increase.

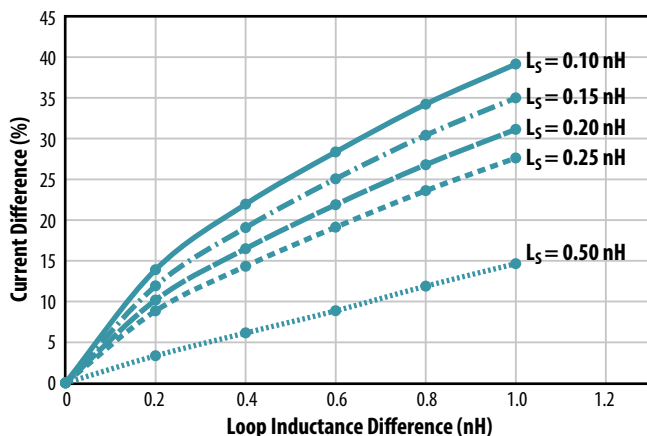


Figure 8: Impact of high frequency loop inductance imbalance on device dynamic current sharing for a $V_{IN} = 48$ V, $I_{OUT} = 25$ A, single phase GaN based buck converter with two half bridges operating in parallel for various common source inductances (GaN transistors: EPC 2001).

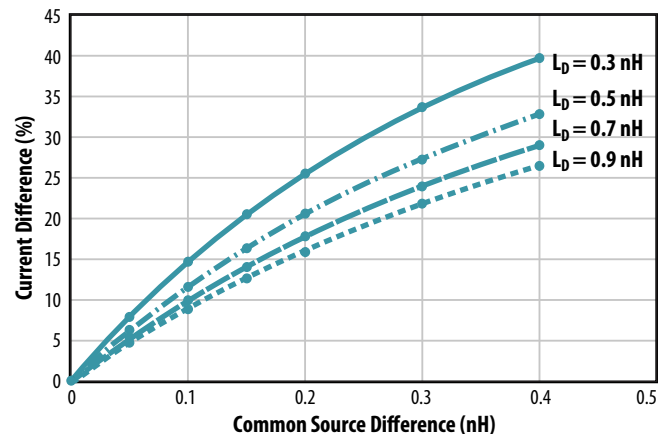


Figure 9: Impact of common source inductance imbalance on device dynamic current sharing for a $V_{IN} = 48$ V, $I_{OUT} = 25$ A, single phase GaN based buck converter with two half bridges operating in parallel for various high frequency loop inductances (GaN transistors: EPC 2001).

B. Optimizing PCB layout for parallel transistors

As switching speeds steadily increase and parasitic inductances continue to decrease, improved techniques must be developed to improve parallel performance. To effectively parallel high speed GaN transistors the parasitic imbalance contributed by the PCB layout must be minimized. We will look at two different parallel layouts based on the optimal layout discussed in the previous section and assess their ability to provide parallel performance similar to an optimized single transistor design. Each half bridge design contains four devices in parallel for the top switch ($T_{1,4}$) and synchronous rectifier ($SR_{1,4}$) and was tested in a single phase buck converter configuration from 48 V to 12 V at a switching frequency of 300 kHz. In total, eight 100 V EPC2001 GaN transistors with a single TI LM5113 gate driver were used to achieve output power up to 480 W and output currents up to 40 A.

The parallel designs are shown in figure 10. In the first design, shown in figure 10 (a), the four GaN transistors are located in close proximity to operate as a “single” power device, with a single high frequency power loop. The drawbacks of this layout are that the high frequency loop inductance will increase as a result of the increased loop size and that devices will have imbalanced parasitics as their individual power loops are different ($L_{loop} \approx 1.7\text{-}2.6$ nH); leading to current sharing and thermal issues. The second design, shown in figure 10 (b) utilizes four distributed high frequency power loops, located symmetrically around the single LM5113 gate driver. The design will provide the lowest overall parasitics for each device pair ($L_{loop} \approx 0.4$ nH) and most importantly, provide the best balancing of the parasitic elements, ensuring proper parallel operation.

The voltage waveforms of the synchronous rectifiers switching transitions for the two designs are also shown in figure 10. For the single high frequency power loop design, the switching node waveforms are shown in figure 10 (a), the voltage transitions for the inner-most and outer-most devices show an almost 2 ns switching time difference, which equates to about 25% of the total switching time. This voltage difference demonstrates the parasitic imbalance in this PCB layout. In the single high frequency loop design, the two devices also exhibit significant voltage overshoot, an effect of the higher

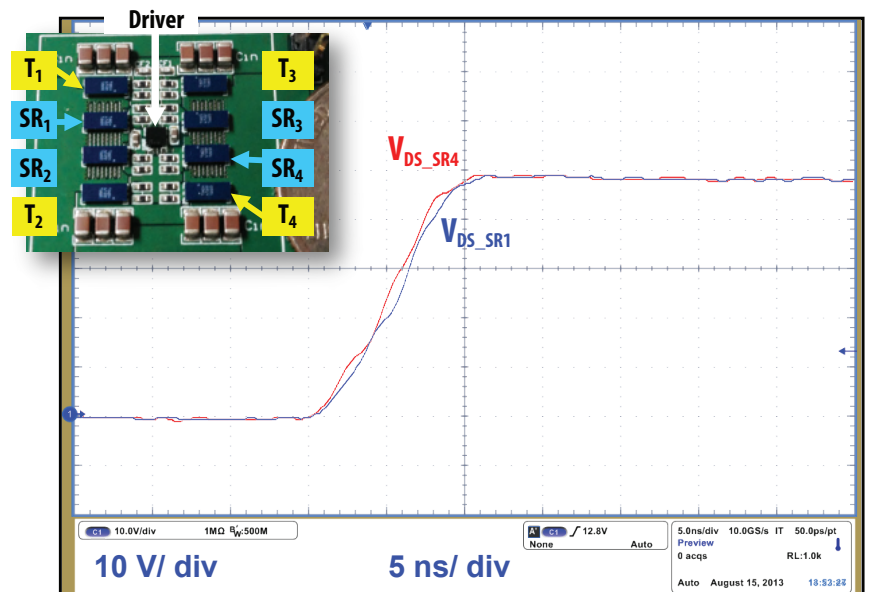
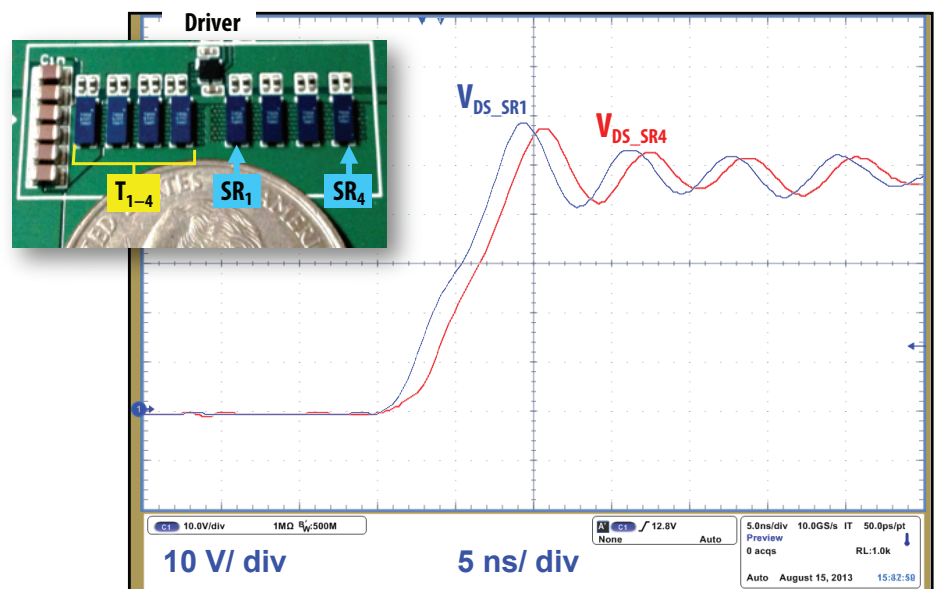


Figure 10: Four parallel GaN half bridge layouts and switching node waveforms with a single high frequency power loop (a) and four distributed high frequency power loops (b) ($V_{in} = 48$ V, $V_{out} = 12$ V, $I_{out} = 30$ A, $f_{sw} = 300$ kHz, GaN transistors T/SR: EPC2001).

individual high frequency loop inductances. The devices also display different voltage overshoots which is also a consequence of the parasitic imbalance.

For the symmetrical four high frequency power loop design the switch-node waveforms are shown in figure 10 (b). The voltage transitions for the devices

are almost identical, demonstrating this layout's ability to balance the parasitics well. The distributed high frequency loop layout also has reduced voltage overshoot, an effect of lower individual high frequency loop inductances. This balanced layout will improve overall performance by offering better electrical and thermal performance.

The thermal evaluations of the two parallel designs are shown in figure 11. A thermal imbalance is evident in the single high frequency loop design, shown in figure 11 (a), where a hot spot develops on the devices handling a greater portion of the power as a result of parasitic imbalance. The top switch closest to the input capacitors, T_1 , has a maximum temperature more than 10°C higher than the top switch furthest away from the input capacitors, T_4 . For the four distributed power loop design, shown in figure 11 (b), there is a very good thermal balance and negligible difference in temperature between the devices. There is also a good distribution of the heat by avoiding clustering of the higher loss top devices on the PCB.

By offering lower individual parasitics and better parasitic balance, the distributed four high frequency loop design has more effective switching and paralleling. This results in better electrical and thermal performance as shown in figure 12. The distributed high frequency loop design offers a 0.2% gain in efficiency at 40 A, and has an almost constant 10°C improvement in the maximum device temperature. The improved four parallel half bridge layout operated as a 48 V to 12 V, 480 W, 300 kHz, 40 A single phase buck converter achieved efficiencies above 96.5% from 35% to 100% load. The ability of GaN transistors to increase switching frequencies, combined with higher power handling capability provided by the effective paralleling methods discussed in this application note allows for the exploration of new opportunities requiring high frequency and high output current.

The switching waveforms for an optimal PCB design with a single GaN transistor, two parallel transistors, and four parallel transistors are shown in figure 13. Looking at the entire switching cycle, as shown in figure 13 (a), the switching speed difference is unnoticeable, demonstrating the ability of parallel GaN transistors to offer high switching speeds for high current applications. Looking at a zoomed view of the switching rise time, as shown in figure 13 (b), the parallel designs effectively operate as a single, larger, lower-resistance device with a slower switching speed in proportion to the number of devices in parallel.

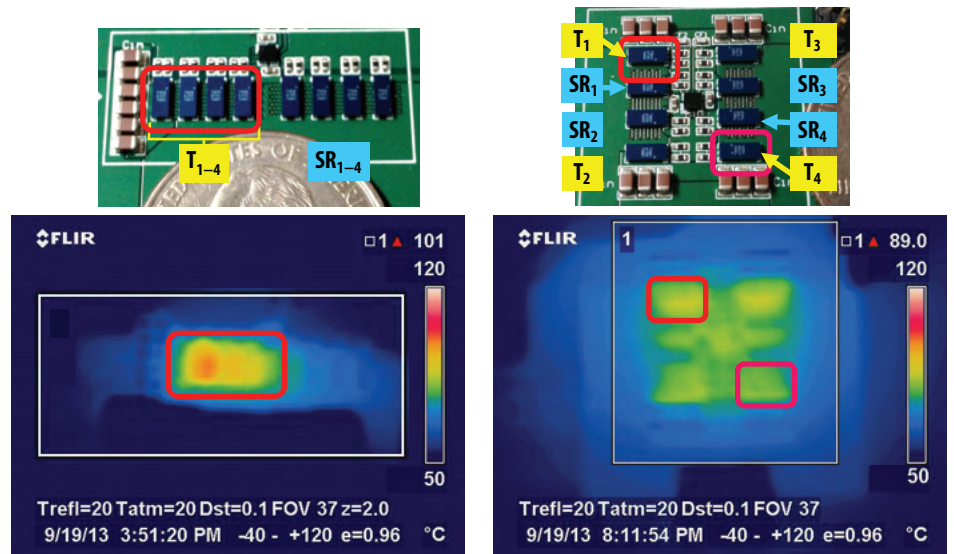


Figure 11: Thermal measurements of parallel GaN half bridge layouts with a single high frequency power loop (a) and four distributed high frequency power loops (b). ($V_{IN} = 48\text{ V}$, $V_{OUT} = 12\text{ V}$, $I_{OUT} = 30\text{ A}$, $f_{sw} = 300\text{ kHz}$, $L = 3.3\ \mu\text{H}$, GaN transistors T/SR: 100 V EPC2001, fan speed: 200 LFM).

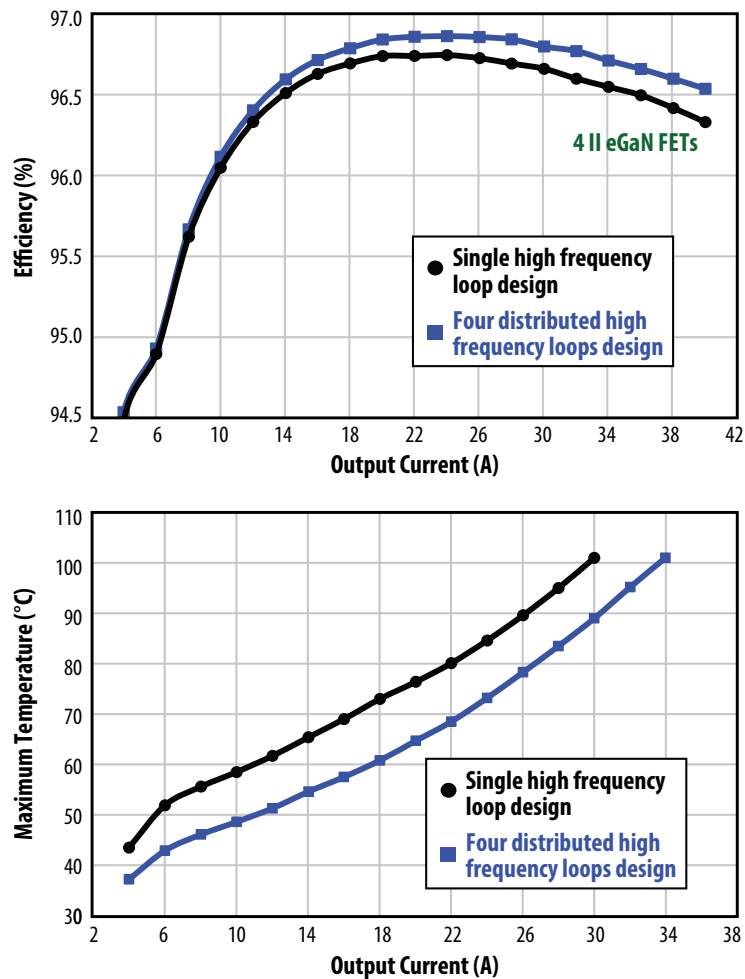


Figure 12: Efficiency (a) and thermal comparison (b) for conventional and proposed parallel GaN half bridge designs ($V_{IN} = 48\text{ V}$, $V_{OUT} = 12\text{ V}$, $f_{sw} = 300\text{ kHz}$, $L = 3.3\ \mu\text{H}$, GaN transistors T/SR: EPC2001).

Conclusions

The introduction of high performance GaN transistors offers the potential to switch at higher frequencies and efficiency than possible with traditional Si MOSFET technology. Combined with improved figures of merit and low parasitic packaging, GaN transistors require a low parasitic PCB layout to fully utilize the device's capability. This work addressed the impact of package and layout parasitics on in-circuit performance and discussed an optimized layout to further enhance the performance capability of GaN transistors. This application note then evaluated the ability to parallel GaN transistors for higher output current applications by addressing the challenges facing paralleling high speed, low parasitic devices and proposing an improved paralleling technique. For experimental verification of the proposed design method, four parallel half bridges in an optimized layout were operated as a 48 V to 12 V, 480 W, 300 kHz, 40 A single phase buck converter and achieved efficiencies above 96.5% from 35% to 100% load.

The proposed design achieved superior electrical and thermal performance compared to conventional paralleling methods and demonstrated that high speed GaN transistors can be effectively paralleled for higher current operation.

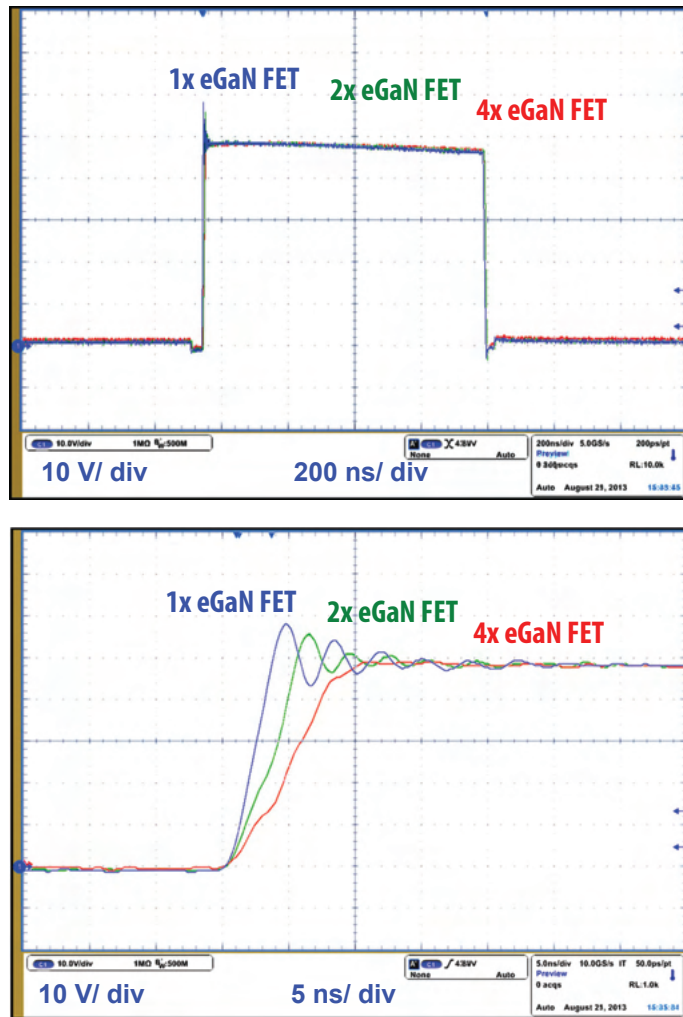


Figure 13: (a) Switching node waveforms with 1, 2 and 4 parallel GaN half bridges (b) zoomed view ($V_{IN} = 48\text{ V}$, $V_{OUT} = 12\text{ V}$, $I_{OUT} = 30\text{ A}/\text{number of GaN FETs}$, $f_{sw} = 300\text{ kHz}$, GaN FET T/SR: 100 V EPC2001).

References:

- [1] A. Lidow, J. Strydom, M. de Rooij, D. Reusch, *GaN Transistors for Efficient Power Conversion*, Second Edition, Wiley, 2014.
- [2] E. O. Johnson, "Physical Limitations on Frequency and Power Parameters of Transistors," RCA, pp. 163-177, 1965.
- [3] R. W. Keyes, "Figure of Merit for Semiconductors for High-Speed Switches," *Proc. IEEE*, p. 225, 1972.
- [4] B. J. Baliga, "Semiconductors for High-Voltage, Vertical Channel FET's," *J. Appl. Phys.* vol. 53, pp. 1759-1764, 1982.
- [5] B. J. Baliga, "Power Semiconductor Device Figure-of-Merit for High Frequency Applications," *IEEE Electron Device Letters*, vol. 10, pp. 455-457, 1989.
- [6] I. J. Kim, S. Matsumoto, T. Sakai, and T. Yachi, "New Power Device Figure-of-Merit for High Frequency Applications," in *Proc. Int. Symp. Power Semiconductor Devices ICs*, Yokohama, Japan, 1995, pp. 309-314.
- [7] A. Q. Huang, "New Unipolar Switching Power Device Figures of Merit," *IEEE Electron Device Letters*, vol. 25, pp. 298-301, 2004.
- [8] Y. Ying, "Device Selection Criteria----Based on Loss Modeling and Figure of Merit," Thesis of Master of Science in Electrical Engineering of Virginia Tech, 2008.
- [9] D. Reusch and J. Strydom, "Evaluation of Gallium Nitride Transistors in High Frequency Resonant and Soft-Switching DC-DC Converters," *Applied Power Electronics Conference and Exposition (APEC)*, pp. 464-470, 2014.
- [10] D. Reusch, D. Gilham, Y. Su, and F. C. Lee, "Gallium Nitride Based 3D Integrated Non-Isolated Point of Load Module," *Applied Power Electronics Conference and Exposition (APEC)*, pp. 38-45, 2012.
- [11] S. Ji, D. Reusch, and F. C. Lee, "High Frequency High Power Density 3D Integrated Gallium Nitride Based Point of Load Module," *Energy Conversion Congress and Exposition (ECCE)*, pp.4267-4273, 2012.
- [12] M. A. de Rooij, "eGaN FET based Wireless Energy Transfer Topology Performance Comparisons", *International Exhibition and Conference for Power Electronics, Intelligent Motion, Renewable Energy and Energy Management (PCIM - Europe)*, pp. 610 - 617, 2014.
- [13] J. Strydom, D. Reusch, "Design and Evaluation of a 10 MHz Gallium Nitride Based 42 V DC-DC Converter," *Applied Power Electronics Conference (APEC)*, pp. 1510-1516. 2014.
- [14] D. Cucak, M Vasić, O Garcia, J.A. Oliver, P. Alou, J.A. Cobos, "Application of eGaN FETs for highly efficient Radio Frequency Power Amplifier," *Integrated Power Electronics Systems, CIPS 2012*, pp.1-6, 2012.
- [15] B. Yang, J. Zhang, "Effect and utilization of common source inductance in synchronous rectification," *Applied Power Electronics Conference and Exposition (APEC)*, pp. 1407-1411, 2005.
- [16] M. Pavier, A. Woodworth, A. Sawle, R. Monteiro, C. Blake, and J. Chiu, "Understanding the effect of power MOSFET package parasitic on VRM circuit efficiency at frequencies above 1 MHz," *PCIM Europe*, pp. 279-284, 2003.
- [17] T. Hashimoto, T. Kawashima, T. Uno, Y. Satou, N. Matsuura, "System in package with mounted capacitor for reduced parasitic inductance in voltage regulators," *Applied Power Electronics Conference and Exposition (APEC)*, pp.187-191, 2008.
- [18] D. Reusch and J. Strydom, "Understanding the Effect of PCB Layout on Circuit Performance in a High Frequency Gallium Nitride Based Point of Load Converter," *Applied Power Electronics Conference (APEC)*, pp.649- 655, 2013.
- [19] J. B. Forsythe, "Paralleling of Power MOSFETs for High Power Output," *International Rectifier Application Note*.
- [20] Y. F. Wu, "Paralleling High-speed GaN Power HEMTs for Quadrupled Power Output," *Applied Power Electronics Conference and Exposition (APEC)*, pp. 211-214, 2013.